

Tight uncertainty relations for cycle currents

Matteo Polettini,^{1,*} Gianmaria Falasco² and Massimiliano Esposito¹

¹*Department of Physics and Materials Science, University of Luxembourg, Campus Limpertsberg, 162a Avenue de la Faïencerie, 1511 Luxembourg, Grand Duchy of Luxembourg*

²*Department of Physics and Astronomy, University of Padova, Via Marzolo 8, 35131 Padova, Italy*



(Received 1 June 2021; revised 11 February 2022; accepted 23 November 2022; published 16 December 2022)

Several recent inequalities bound the precision of a current, i.e., a counter of the net number of transitions in a system, by a thermodynamic measure of dissipation. However, while currents may be defined locally, dissipation is a global property. Inspired by the fact that, ever since Carnot, cycles are the unit elements of thermodynamic processes, we prove similar bounds tailored to cycle currents, counting net cycle completions, in terms of their conjugate affinities. We show that these inequalities are stricter than previous ones, even far from equilibrium, and that they allow us to tighten those on transition currents. We illustrate our results with a simple model and discuss some technical and conceptual issues related to shifting attention from transition to cycle observables.

DOI: [10.1103/PhysRevE.106.064121](https://doi.org/10.1103/PhysRevE.106.064121)

I. INTRODUCTION

In recent years several variants of a thermodynamic uncertainty relation (TUR) have been derived, bounding the precision of an observable by a quantity of clear physical interpretation. In particular, one-half of the mean entropy flow rate is an upper bound to the squared signal-to-noise ratio of any stationary thermodynamic current ϕ_a . We can cast this as a bound on the current's dispersion

$$D_a^\infty = \frac{\kappa_a^{(2)}}{|\kappa_a^{(1)}|} \geq \frac{2}{\sigma/|\kappa_a^{(1)}|} \quad (1)$$

in terms of the current's mean $\kappa_a^{(1)}$ and variance $\kappa_a^{(2)}$, scaled over long times $t \rightarrow +\infty$. The entropy flow rate $\sigma = \sum_a F_a \kappa_a^{(1)}$ accounts for all physical mechanisms that affect the system, weighted by their affinities F_a , which we assume to be fixed and known. In other words, precision costs: The more precise the current, the greater the dissipation.

A common framework to prove this and similar results is that of discrete-state space, continuous-time stationary Markov walks [1–6]. In this case, by current conservation, observables are associated with cycles inside the system's state space (see, e.g., Ref. [7]). Large-deviation and information theories allow unified formulations: In particular, TURs for observables that are odd under an involution (e.g., time reversal) follow from the Hilbert structure of the space of observables [8]. The bound (1) saturates close to equilibrium if the current is the entropy flow itself [9]. Other derivations encompass periodic states [10] and relaxation [4,11–13], possibly non-Markovian and subject to feedback, as well as time-symmetric observables and first-passage times [14–16].

Thermodynamic uncertainty relations are more meaningful the tighter they are. Pursuing a line of research that aims at

casting global results as local [17–19], in this paper we show how to produce tighter bounds on the currents. The key insight is to shift attention from transition currents $a = x'x$ (counting net transitions from a state x to another x') to cycle currents $a = c$ (from a state back to itself via cycle c). One of several possible procedures to define a set of cycle currents along a realization of the Markov walk is illustrated in Fig. 1 and can be told in terms of an ancient Greek myth. Suppose the Markov walker is Theseus, wandering around the Knossos labyrinth to find and kill the Minotaur. In our thermodynamic twist of the story, as Theseus lays Ariadne's thread, to save resources, whenever he accidentally encounters the filament he laid, he cuts it, wraps up the thread behind him, and sews the strand's ends together, labeling the cycle he performed and bookkeeping the number of its completions (later on Theseus may traverse the same cycle again).

Cycle currents are the net number of times a cycle without crossings is performed as listed in Theseus's parchment with respect to some orientation (e.g., clockwise or counter-clockwise). They are a truly different kind of observable with respect to transition currents, even including Schnakenberg's. In particular, they have a long-time memory, as is already evident from our illustration: Cycle γ was recorded by Theseus after β , but it actually was initiated earlier.

Our main result then is

$$D_c^0(t) \geq \frac{2}{F_c}, \quad (2)$$

where the superscript 0 indicates instantaneous estimates at any given time t , independently of the starting state. Equation (2) holds for the joint dispersion of all cycle currents that produce the same affinity. Note that this equation is analogous to Eq. (1) when only one mechanism contributes to the entropy flow (see Ref. [20] for other cases where the right-hand side is simplified). In our case, though, the network can be multicyclic.

*matteo.polettini@uni.lu

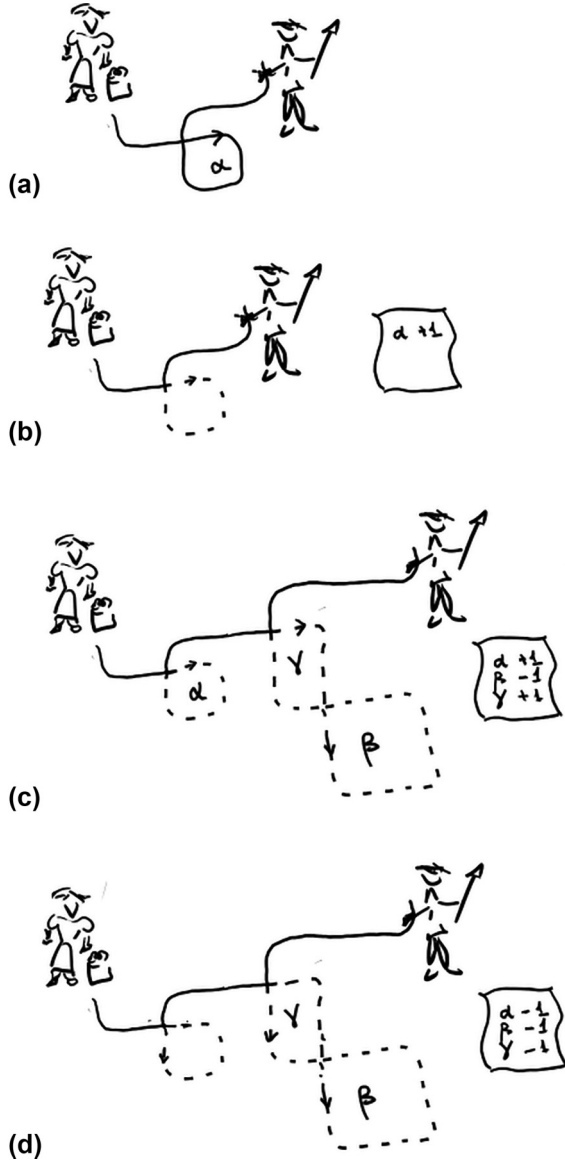


FIG. 1. (a) First cycle α walked by Theseus in the clockwise direction. (b) Strand removed and the cycle recorded. (c) More cycles recorded. Notice that β is in the counterclockwise direction and that γ was started before β but is completed after. (d) Partial inversion of cycles α and γ .

As a second result, we tighten the stationary bound (1) for transition currents $a = x'x$ by replacing σ with $\sigma_{x'x} \leq \sigma$, a reduced measure of the mean entropy flow rate along all cycles that contain transition $x'x$. Finally, we provide some computational evidence for the long-time analog of Eq. (2), $D_c^\infty \geq 2/F_c$. However, a proof of the latter relation remains elusive and poses interesting mathematical and conceptual questions.

II. SETUP

Thermodynamics deals with time-integrated currents $\phi_a(t_0, t)$ measured in an interval $[t_0, t]$. Currents are powered by conjugate forces F_a ; without loss of generality, we let all $F_a > 0$. The entropy flow $\Sigma := \sum_a F_a \phi_a$ quantifies

dissipation. In the stochastic framework currents are random variables, functionals $\phi_a(t_0, t) = \phi_a[\omega]$ of stochastic paths ω which we assume to be continuous-time stationary Markov walks on state space $X \ni x$, with time-independent rates $r_{x'x} > 0$ of jumping from x to x' . We assume microscopic reversibility: $r_{x'x} > 0 \Rightarrow r_{xx'} > 0$. A path is a succession of visited states x_i and sojourn times τ_i up to total time $\sum_{i=0}^n \tau_i = t - t_0$,

$$\omega = (x_0, \tau_0) \rightarrow (x_1, \tau_1) \rightarrow \cdots \rightarrow (x_n, \tau_n), \quad (3)$$

where n is the total number of jumps, itself a random variable. A probability density of the path compatible with the currents' statistics is given by

$$p(\omega) = e^{-r_{x_n} \tau_n} \left(\prod_{i=0}^{n-1} r_{x_{i+1}x_i} e^{-r_{x_i} \tau_i} \right) p_{t_0}(x_0), \quad (4)$$

where $r_x = \sum_{x'} r_{x'x}$ is the exit rate out of a state and $p_{t_0}(x_0)$ is the distribution of the initial state. Currents are assumed to be antisymmetric $\phi_a[\omega] = -\phi_a[\bar{\omega}]$ by time reversal of the path, defined as $\bar{\omega} := (x_n, \tau_n) \rightarrow \cdots \rightarrow (x_1, \tau_1) \rightarrow (x_0, \tau_0)$. We focus on their mean and variance

$$K_a^{(1)}(t_0, t) := \langle \phi_a(t_0, t) \rangle, \quad (5)$$

$$K_a^{(2)}(t_0, t) := \langle [\phi_a(t_0, t) - \langle \phi_a(t_0, t) \rangle]^2 \rangle,$$

where $\langle \cdot \rangle$ is the expected value with respect to $p(\omega)$. In particular, we are interested in the stationary and the instantaneous dispersions

$$D_a^{\infty/0}(t_0) := \lim_{t \rightarrow +\infty/t_0} \frac{K_a^{(2)}(t_0, t)}{K_a^{(1)}(t_0, t)}. \quad (6)$$

The first is independent of the initial time $D^\infty(t_0) = D^\infty$ and converges to a finite value, due to the fact that all cumulants of the currents are time extensive $K_a^{(j)}(t_0, t)/(t - t_0) \xrightarrow{t \rightarrow +\infty} \kappa_a^{(j)}$, which in turn follows from the existence of a large-deviation principle. While this is well known for transition currents, for cycle currents this was established by Theorem 5 in Ref. [21]. The above transition TUR (1) then follows in terms of the transition forces $F_{x'x} := \ln r_{x'x}/r_{xx'}$.

III. CYCLE CURRENTS AND INVOLUTIONS

Let \mathcal{C} be the set of all simple cycles of the graph, i.e., directed and without overlaps. The first ingredient in our derivation is the decomposition of path ω as a sequence of simple cycles $c \in \mathcal{C}$. Let $-c$ denote the cycle with direction opposite to $+c = c$. For both cycle directions we introduce cycle fluxes $\psi_{\pm c}[\omega]$ and their antisymmetric part, the cycle currents $\phi_c[\omega] := \psi_{+c}[\omega] - \psi_{-c}[\omega]$, as defined by the following procedure. Consider that one (of many) cycle decomposition of a path follows the suggestion in Fig. 1. As the path unfolds, we look at the first state that occurs twice, at transitions numbered k and k' . Then the states $x_k \rightarrow x_{k+1} \rightarrow \cdots \rightarrow x_{k'}$ form a simple cycle $+c$:

$$\cdots \rightarrow \overbrace{(x_k, \tau_k) \rightarrow (x_{k+1}, \tau_{k+1}) \rightarrow \cdots \rightarrow (x_{k'} \equiv x_k, \tau_{k'})}^{+c} \rightarrow \cdots \quad (7)$$

Every time one such cycle is identified we increase the corresponding cycle flux by one unit and then remove the

corresponding transitions from the path, yielding

$$\dots \rightarrow (x_{k'}, \tau_{k'}) \rightarrow \dots \quad (8)$$

We proceed like this until we are left with a “stump,” that is, a piece of path from x_0 to x_n that contains no cycles. If the path is closed $x_0 \equiv x_n$, then the stump consists of (x_n, τ_n) only.

We can now create a partial reversal of the path by flipping the direction of cycle $\pm c$ into $\mp c$ whenever it occurs, e.g.,

$$\dots \rightarrow \overbrace{(x_{k'}, \tau_{k'}) \rightarrow (x_{k'-1}, \tau_{k'-1}) \rightarrow \dots \rightarrow (x_k, \tau_k)}^{-c} \rightarrow \dots \quad (9)$$

Proceeding in a similar manner for all cycles in a given subset $\mathcal{C}' \subseteq \mathcal{C}$ we obtain a new path $\tilde{\omega}$, which we call the partially reversed path [see Fig. 1(d)]. Note that cycle currents $\phi[\omega] = \{\phi_c[\omega]\}_{c \in \mathcal{C}'} = -\phi[\tilde{\omega}]$ are antisymmetric by partial reversal.

Now consider $p(\tilde{\omega})$, where we sample the initial state with the same probability $p_0(x_0)$, given that the stump is not affected by partial reversal. Also, the waiting-time distribution at states is exactly the same as in the forward path. Finally, all transitions not belonging to the cycle will also be in the same direction. Therefore, the fluctuation relation

$$\frac{p(\phi[\omega])}{p(-\phi[\omega])} = \frac{p(\omega)}{p(\tilde{\omega})} = \exp \sum_{c \in \mathcal{C}'} F_c \phi_c[\omega] \quad (10)$$

holds, where we introduced the cycle affinity

$$F_c := \sum_{x'x \in c} F_{x'x} = \ln \prod_{x'x \in c} \frac{r_{x'x}}{r_{xx'}}. \quad (11)$$

Importantly, the above fluctuation relation holds exactly at all times and does not require the long-time limit.

IV. EXPONENTIAL RELATION FROM HILBERT-SPACE STRUCTURE

The second crucial ingredient in our derivation is the Hilbert-space approach to uncertainties of Ref. [8]. We consider the space $\mathcal{H}_{\mathcal{C}'}$ of square-integrable functions that are odd under partial time reversal $\omega \rightarrow \tilde{\omega}$, endowed with the scalar product $\langle f|g \rangle := \sum_{\omega} p(\omega) f(\omega) g(\omega)$. Defining $\tilde{p}(\omega) := p(\tilde{\omega})$ and using the antisymmetry, one finds that the observable $m = (p - \tilde{p})/(p + \tilde{p})$, living in the dual space $\mathcal{H}_{\mathcal{C}'}$, takes averages $\langle f \rangle = \langle m|f \rangle$ for all $|f \rangle \in \mathcal{H}_{\mathcal{C}'}$. Then the variance of f is $\langle f|f \rangle - \langle m|f \rangle^2$ and the Cauchy-Schwarz inequality $\langle m|f \rangle^2 \leq \langle m|m \rangle \langle f|f \rangle$ yields

$$\frac{\langle f|f \rangle - \langle f \rangle^2}{\langle f \rangle^2} \geq \frac{1 - \langle \tanh \frac{s}{2} \rangle}{\langle \tanh \frac{s}{2} \rangle} \geq \frac{2}{\exp(s) - 1}, \quad (12)$$

where $s := \ln p/\tilde{p}$ and in the last inequality we used the fact that $\langle \tanh \frac{s}{2} \rangle \leq \tanh(\frac{s}{2})$ [8].

Proof. Defining the probability $p^+ = (p - \tilde{p})/2N$ for $s > 0$ and zero otherwise, with N a proper normalization, we have that $\langle \tanh s/2 \rangle = N \langle \tanh s/2 \rangle^+ \leq N \tanh \langle s/2 \rangle^+ = N \tanh \langle s/2N \rangle$, where we used the Jensen inequality on concave functions. One concludes by noticing that the latter is a strictly increasing function of N and that $N < 1$. ■

In view of the fluctuation relation (10), we then find for an arbitrary linear combination $\phi_a = \sum_{c \in \mathcal{C}'} a_c \phi_c$ of observable

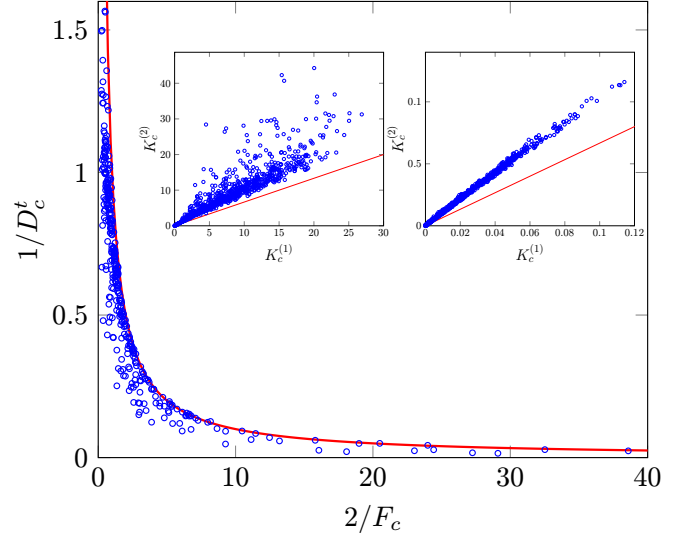


FIG. 2. Randomization over transition rates uniformly distributed in $(0,10)$, inverse of the dispersion $1/D_c^t(t_0)$ of the current of cycle $c = 1 \rightarrow 2 \rightarrow 3 \rightarrow 1$ in the four-state model depicted in Eq. (15), over a time interval $|t - t_0| = 10^2$, long with respect to the average jump time, as a function of twice the inverse of F_c . Data points are obtained via numerical simulation with the Gillespie algorithm. The current is obtained by counting the net completion number of the cycle, where permutations of the cycle are counted together. Mean and variance are then calculated averaging over 10^4 different realizations. The red solid line corresponds to the equation $y = 1/x$. The insets show the variance versus mean obtained by randomizing over transition rates at fixed cycle affinity $F_c = 3$. The path duration is $|t - t_0| = 1$ (left) and $|t - t_0| = 10^2$ (right). The symbols' size is of the order of the estimated standard error. Red lines have slope $2/F_c$.

cycle currents the exponential bound

$$\frac{K_a^{(2)}(t_0, t)}{K_a^{(1)}(t_0, t)^2} \geq \frac{2}{\exp \sum_{c \in \mathcal{C}'} F_c K_c^{(1)}(t_0, t) - 1}. \quad (13)$$

V. INSTANTANEOUS BOUND ON CYCLE CURRENT

We are finally in the position to formulate our first main result. We consider short paths in the time interval $[t, t + \delta t]$. Because transition fluxes are linear combinations of cycle fluxes up to the stump and both are positive, and given that the former's average is of order δt , we know (as intuitive) that mean cycle currents are at most of order δt .¹ Then we can linearize the exponential in Eq. (12):

$$\frac{K_a^{(2)}(t, t + \delta t)}{K_a^{(1)}(t, t + \delta t)^2} \geq \frac{2}{\sum_{c \in \mathcal{C}'} F_c K_c^{(1)}(t, t + \delta t)} + o(\delta t^2). \quad (14)$$

In particular, selecting the family of currents $a = c$ that have affinity F_c and taking the limit $\delta t \rightarrow 0$, we arrive at the bound introduced in Eq. (2). In Fig. 2 we study numerically the extension of Eq. (2) to two different finite times, one

¹In fact, we verified numerically that they are sublinear for small δt , due to the fact that it takes more than one transition to complete a cycle.

large and one small with respect to the system's relaxation timescales (respectively approximating the instantaneous and the asymptotic bounds), both at fixed affinity (insets), and also randomizing over all affinities (main figure), on one of the three simple cycles of the four-state model

$$\begin{array}{|c|c|} \hline 1 & 2 \\ \hline & \diagup \\ \hline 4 & 3 \\ \hline \end{array}; \quad \mathcal{C} = \left\{ \begin{array}{|c|} \hline \diagup \\ \hline \end{array}, \begin{array}{|c|} \hline \diagdown \\ \hline \end{array}, \begin{array}{|c|} \hline \square \\ \hline \end{array} \right\}. \quad (15)$$

VI. CYCLE BOUNDS FOR TRANSITION CURRENTS

By construction, the number of times transition $x'x$ occurs equals the number of times some cycle through $x'x$ occurs [21]. Therefore, we have

$$\phi_{x'x}(t_0, t) = \sum_{c \in \mathcal{C}_{x'x}} \phi_c(t_0, t) + \theta_{x'x}(t_0, t), \quad (16)$$

where $\mathcal{C}' \equiv \mathcal{C}_{x'x}$ are all simple oriented cycles that contain transition $x'x$ and $\theta_{x'x}(t_0, t)$ accounts for time-inextensive occurrences in the stump. The latter term is bounded, and in fact in the stationary limit it can be disregarded both on average and from the determination of all the cumulants of the edge current.

Proof. A single edge current's rate function can be obtained by the contraction principle from that of all edge currents, and thus it inherits their symmetries. Edge currents separated by a so-called cocycle current (the current supported on any of the edges that separate the graph in two disjoint subsets) are well known to have the same rate function and thus the same long-time statistics [22]. On the other hand, by continuity of the stump, the term $\theta_{x'x}(t_0, t)$ can only contribute ± 1 or 0 to the one specific cocycle containing edge $x' \leftarrow x$; thus $\sum_{c \in \mathcal{C}_{x'x}} \phi_c(t_0, t)$ is statistically equivalent to $\phi_{x'x}(t_0, t)$. ■

Plugging Eq. (16) into the entropy flow and swapping the sum over transitions and that over cycles, we find as an important consistency check that cycle currents are thermodynamically consistent, meaning that, by definition of cycle affinity,

$$\Sigma \approx \sum_{x' < x} F_{x'x} \sum_{c \in \mathcal{C}_{x'x}} \phi_c = \sum_{c \in \mathcal{C}} F_c \phi_c, \quad (17)$$

where \approx stands for asymptotically in the long-time limit. Because of the long-time limit and by Eq. (16), we can consider the transition case $a \equiv x'x$ in Eq. (13). Importantly, transition currents are time additive along paths, $\phi_{x'x}(t_0, t_2) = \phi_{x'x}(t_0, t_1) + \phi_{x'x}(t_1, t_2)$ for $t_0 < t_1 < t_2$. This unlocks another argument in the derivation of Ref. [8], assuming that the system has already relaxed to a stationary state $t_0 \rightarrow \infty$. Viewing this as a periodic state with period δt , the minimum (over the set of square-integrable functions that are odd under time reversal) variance over the squared mean in the time span $t - t_0$ is bounded by $1/N = \delta t/(t - t_0)$ times the minimum variance over the squared mean in the time interval δt . Namely, in view of Eq. (14),

$$\frac{K_{x'x}^{(2)}(t_0, t_0 + N\delta t)}{K_{x'x}^{(1)}(t_0, t_0 + N\delta t)^2} \geq \frac{2}{N \sum_{c \in \mathcal{C}_{x'x}} F_c K_c^{(1)}(t, t + \delta t)}, \quad (18)$$

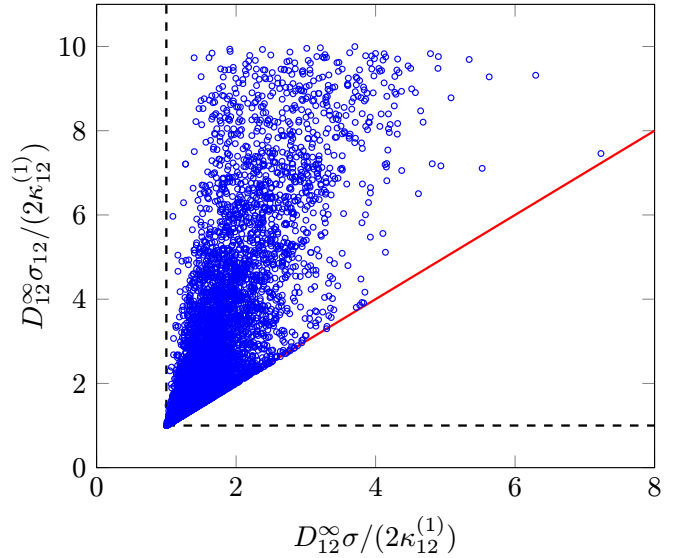


FIG. 3. Scatter plot of $D_{12}^{\infty} \sigma_{12} / (2\kappa_{12}^{(1)})$ in terms of $D_{12}^{\infty} \sigma / (2\kappa_{12}^{(1)})$ for systems with randomized rates in the unit interval, showing that both bounds are satisfied (all points are above the $x = 1$ and $y = 1$ axes, dashed lines) and that the local bound performs better than the global one (all points are above the $x = y$ line, red solid line).

when we let $\delta t \rightarrow 0$ and $N \rightarrow \infty$ at fixed and arbitrarily large $t - t_0$. Defining $\sigma_{x'x} := \sum_{c \in \mathcal{C}_{x'x}} F_c \kappa_c^{(1)}$ and using Eq. (13) to bound the right-hand side of Eq. (18), we arrive at

$$D_{x'x}^{\infty} \geq \frac{2}{\sigma_{x'x} / |\kappa_{x'x}^{(1)}|}. \quad (19)$$

To compute $\sigma_{x'x}$, we use the known [23,24] analytical expression for the mean stationary cycle currents $\kappa_c^{(1)} = S_c (P_c^+ - P_c^-)$. Here P_c^{\pm} is the product of rates in the clockwise or counterclockwise directions along the cycle, respectively, while S_c is a positive factor, symmetric by reversal of the cycle [24]. Because $F_c = \ln P_c^+ / P_c^-$ and $(x - y) \ln x / y \geq 0$, we find that each term in $\sigma_{x'x}$ is non-negative. Furthermore, given Eq. (17), because we are summing over a subset of all simple cycles, we have that $\sigma_{x'x} \leq \sigma$. Therefore, the latter bound improves on the global one. We illustrate this result in Fig. 3.

VII. DISCUSSION

While extensive in time, cycle currents are not additive. For this reason, several results known for transition currents do not immediately apply to cycle currents because of memory effects. Due to that, we were not able to prove the long-time-averaged uncertainty relation, namely, Eq. (2) but with 0 replaced by $+\infty$. In the simulations sustaining it (see Fig. 2 as well as the right inset), while we were cautious about self-correlation and relaxation errors already present in Markov chain Monte Carlo algorithms [25], due to autocorrelations, cycle currents may introduce specific systematic errors that need to be investigated further.

Regarding the improved bound on transition currents, as the system size grows, the number of cycles containing one particular transition grows more slowly than the total number of cycles. For example, in a complete graph with V vertices

there are $\sum_{k=3}^V V!/(V-k)!2k$ simple cycles, while the number of cycles through a particular transition (not counting the trivial cycle between two nodes) is $\lfloor * \rfloor (V-2)!e - 1$: For the first few values of $V \geq 3$ the ratios of local-to-global cycles are 1, 4/7, 15/37, 64/197, 325/1172, and 978/4009. Furthermore, the factor S_c is typically smaller the larger the cycle is. All of this indicates that in larger systems local cycle bounds on transition currents may perform enormously better than global ones. In more general cases the number $n(C)$ of simple cycles for a graph with cyclomatic number $C = E - V + 1$ (transitions minus vertices plus one) is $2^C - 1 \geq n(C) \geq 2^{C-1} + C^2 - 3C + 3$ and usually the lower bound is a good approximation [26]. Estimates on the number of cycles sharing a given transition are not known, but since a cyclomatic number of simple basis cycles is sufficient to compose any simple cycle and since the basis cycles that compose a given simple cycle must be adjacent to one another, simple cycles could be viewed as walks in the dual graph or matroid and such estimates may be mapped into known walk-enumeration problems. Finally, when considering not just the bare cycle number but the dissipation each cycle provides, assuming the rates to be homogeneously distributed over the graph, the factor S_c has a tendency to become smaller the larger cycle c is, that is, the further away it goes from the rooting vertex, due to the fact that this factor measures the contraction of the number of spanning trees upon identification of the cycle with a unique vertex [24].

VIII. CONCLUSION

Note that while Theseus is a comoving (Lagrangian) observer along the whole trajectory, we could also think of a stationary (Eulerian) observer that “sits” on a specific cycle, of which he monitors each and every passage of Theseus and is ignorant of whatever happens in the rest of the network. That is, between two successive transitions along a cycle there might be detours, but note that as such detours necessarily complete a cycle for the next transition to occur, these do not influence the definition of the cycle currents and

the above relations hold by construction, given that all other cycles are marginalized in the path integrals (such “drag and drop” processes have been discussed at length in Ref. [27]). Cycle currents may then serve as interesting observables for a local formulation of thermodynamics. Note the give and get: In order to go more local in the overall description (e.g., of the dissipation bounding the precision of the current along one specific transition), one needs to consider a less-local observable (in fact, relevant cycles will in any case span the whole system).

From an operational point of view, focusing on cycle currents requires a substantial shift, from an external observer that monitors the flows to and from all possible reservoirs to an internal observer that records the story of a local process. This approach may then be relevant when considering processes which go through an ordered sequence of events to be completed, in analogy to a product that goes through different stages along a factory line [28]. Furthermore, similar situations arise when a cell undergoes a well-defined sequence of transformations before dividing [29]. From a more speculative standpoint, one might argue that in situations where it is difficult to clearly separate a specific system’s externalities from those of other systems, in place of observables related to the estimation of the global energy demand and supply, local observables related to specific cycles may be the *only* viable thermodynamic observables. Apart from a few seminal works [21,30], some applications to cycle-completion time statistics [31,32], and a recent large-deviation treatment [33] (which employs a counting procedure not equivalent to ours), little is known about the mathematics of these observables.

ACKNOWLEDGMENTS

This research was supported by the National Research Fund Luxembourg (Project CORE ThermoComp, No. C17/MS/11696700) and by the European Research Council, Project NanoThermo (ERC-2015-CoG Agreement No. 681456). G.F. is funded by the European Union – NextGenerationEU – and by the program STARS@UNIPD with the project “ThermoComplex”.

-
- [1] A. C. Barato and U. Seifert, *Phys. Rev. Lett.* **114**, 158101 (2015).
 - [2] P. Pietzonka, A. C. Barato, and U. Seifert, *J. Stat. Mech.* (2016) 124004.
 - [3] T. R. Gingrich, J. M. Horowitz, N. Perunov, and J. L. England, *Phys. Rev. Lett.* **116**, 120601 (2016).
 - [4] P. Pietzonka, F. Ritort, and U. Seifert, *Phys. Rev. E* **96**, 012101 (2017).
 - [5] T. R. Gingrich, G. M. Rotskoff, and J. M. Horowitz, *J. Phys. A: Math. Theor.* **50**, 184004 (2017).
 - [6] J. M. Horowitz and T. R. Gingrich, *Phys. Rev. E* **96**, 020103(R) (2017).
 - [7] J. Schnakenberg, *Rev. Mod. Phys.* **48**, 571 (1976).
 - [8] G. Falasco, M. Esposito, and J.-C. Delvenne, *New J. Phys.* **22**, 053046 (2020).
 - [9] M. Polettni, A. Lazarescu, and M. Esposito, *Phys. Rev. E* **94**, 052104 (2016).
 - [10] K. Proesmans and C. Van den Broeck, *Europhys. Lett.* **119**, 20001 (2017).
 - [11] A. Dechant and S.-i. Sasa, *J. Stat. Mech.* (2018) 063209.
 - [12] Y. Hasegawa and T. Van Vu, *Phys. Rev. Lett.* **123**, 110602 (2019).
 - [13] A. Dechant and S.-i. Sasa, *Proc. Natl. Acad. Sci. U.S.A.* **117**, 6430 (2020).
 - [14] J. P. Garrahan, *Phys. Rev. E* **95**, 032134 (2017).
 - [15] T. R. Gingrich and J. M. Horowitz, *Phys. Rev. Lett.* **119**, 170601 (2017).
 - [16] I. Di Terlizzi and M. Baiesi, *J. Phys. A: Math. Theor.* **52**, 02LT03 (2019).
 - [17] M. Polettni and M. Esposito, *J. Stat. Phys.* **176**, 94 (2019).

- [18] G. Bisker, M. Polettini, T. R. Gingrich, and J. M. Horowitz, *J. Stat. Mech.* (2017) 093210.
- [19] I. A. Martínez, G. Bisker, J. M. Horowitz, and J. M. Parrondo, *Nat. Commun.* **10**, 1 (2019).
- [20] A. C. Barato and U. Seifert, *J. Phys. Chem. B* **119**, 6555 (2015).
- [21] C. Jia, D.-Q. Jiang, and M.-P. Qian, *Ann. Appl. Probab.* **26**, 2454 (2016).
- [22] A. Wachtel, J. Vollmer, and B. Altaner, *Phys. Rev. E* **92**, 042132 (2015).
- [23] D.-Q. Jiang, M. Qian, and M.-P. Qian, *Mathematical Theory of Nonequilibrium Steady States: On the Frontier of Probability and Dynamical Systems*, Lecture Notes in Mathematics Vol. 1833 (Springer, Berlin, 2004), pp. 11–44.
- [24] R. Zia and B. Schmittmann, *J. Stat. Mech.* (2007) P07012.
- [25] A. Sokal, in *Functional Integration*, edited by C. DeWitt-Morette, P. Cartier, and A. Folacci, NATO Advanced Studies Institute, Series B: Physics (Springer, Boston, 1997), Vol. 361, pp. 131–192.
- [26] R. Entinger and P. Slater, *Ars Combin.* **11**, 289 (1981).
- [27] M. Bauer and F. Cornu, *J. Stat. Phys.* **155**, 703 (2014).
- [28] M. D. Pandey and J. Van Der Weide, *Struct. Saf.* **67**, 27 (2017).
- [29] M. Ahmadian, J. J. Tyson, J. Peccoud, and Y. Cao, *NPJ Syst. Biol. Appl.* **6**, 7 (2020).
- [30] S. L. Kalpazidou, *Cycle Representations of Markov Processes, Stochastic Modelling and Applied Probability* Vol. 28 (Springer Science + Business Media, New York, 2007).
- [31] H. Qian and X. S. Xie, *Phys. Rev. E* **74**, 010902(R) (2006).
- [32] H. Ge, *J. Phys. Chem. B* **112**, 61 (2008).
- [33] P. Pietzonka, J. Guioth, and R. L. Jack, *Phys. Rev. E* **104**, 064137 (2021).